

Influence of tissue particles on Fas expression in idiopathic interstitial pneumonia

Y Shimizu^{1,2}, S Matsuzaki¹, T Satoh³, T Ohkubo³, A Yokoyama³, Y Ishii³, T Kamiya³, K Arakawa³, K Shimizu^{K4}, Tanaka S⁵, Mori M¹, K Dobashi⁶

¹Department of Medicine and Molecular Science, Gunma University Graduate School of Medicine, Maebashi Gunma Japan,

²WHO Collaborating Center of Prevention and Control of Chronic Respiratory Diseases, Dokkyo University, (DU-WCC), Mibu Tochigi, Japan, ³Japan Atomic Energy Agency, Takasaki Advanced Radiation Research Institute, Takasaki, Gunma, Japan,

⁴Division of Thoracic and Visceral Organ Surgery, Gunma University Graduate School of Medicine, Maebashi, Gunma, Japan,

⁵Department of General Surgical Science, Gunma University Graduate School of Medicine, Maebashi Gunma, Japan, ⁶Gunma University Faculty of Health Science, Maebashi Gunma, Japan

TABLE OF CONTENTS

1. Abstract

2. Introduction

2.1. in-air micro-PIXE analysis system

3. Methods

3.1. Patients and sample preparation

3.2. In-air micro-PIXE system

3.3. Immunohistochemistry

3.4. Calculation of the content of elements

3.5. Statistical analysis

4. Results

4.1. Detection of particles

4.2. Quantitative analysis of Si and Fe and the co-localization of particles with Fas expressions

5. Discussion

5.1. Si and Fe were detected both in IIP and non-IIP lung tissues

5.2. Co-localization of particle depositions and Fas expressions in lung of IIP patients

5.3. Fe deposition in lung tissue

5.4. Limitations of this study

6. Acknowledgements

7. References

1. ABSTRACT

Idiopathic interstitial pneumonia (IIP) is a progressive fibrosing interstitial pneumonia of unknown etiology with a poor prognosis. The aim of this study is to prove the occurrence of particle deposition and particle-induced tissue damage in IIP by examining proapoptotic Fas expression with in-air microparticle induced X-ray emission (in-air micro-PIXE) analysis. A total of 21 patients were enrolled. Lung tissues from 12 IIP patients and nontumorous lung tissues from 9 lung cancer patients (as a control) were subjected to in-air micro-PIXE analysis. The distribution of particles in lung tissue was compared with the localization of Fas expression by immunohistochemistry. Silicon (Si) was identified in 58.3% of IIP samples and 44.4% of control samples. Iron (Fe) was identified 25% in IIP samples and 11.1% in control samples. The mean lung tissue content of Si and Fe relative to S did not differ between IIP and control patients. Only two IIP patients showed the co-localization of Si and Fe deposition with Fas expression. Adaptation of this method would contribute to assess the influence of particles on IIP

2. INTRODUCTION

Idiopathic interstitial fibrosis (IIP) is a heterogeneous disease complex of unknown etiology. Interstitial pneumonia occurs in patients with pathological classification of usual interstitial pneumonia (UIP) in idiopathic pulmonary fibrosis (IPF) or fibrotic-non specific interstitial pneumonia (f-NSIP), so that a differential diagnosis needs to be made from other interstitial pneumonias caused by collagen vascular diseases, asbestosis, or hypersensitivity pneumonitis. Many hypotheses have been discussed with regard to the pathogenesis of IIP, and occupational and environmental factors are thought to act as triggers or risk factors for this condition (1). In a previous study of surgical lung biopsy specimens from 1,311 IPF autopsy cases, the rate of IPF was more than two-fold higher in persons exposed to dust or organic matter than in persons who had other occupations. In that study, examination of surgical lung biopsy specimens from 86 living subjects showed that metal workers and miners had a significantly higher risk of IPF (2). In a questionnaire survey about environmental exposure and IPF, metal dust exposure (among

PIXE analysis of tissue particles in IIP

occupational agents) and cigarette smoking (20.0 to 39.9 pack-years) were particularly associated with a higher risk of IPF (3). Meta-analysis of studies about the etiology of IPF has shown that exposure to smoking, agriculture/farming, livestock, wood dust, and stone/sand is significantly associated with IPF (4). Thus, occupational and environmental factors are regarded as increasing the susceptibility to IPF, but there are limitations to the data obtained by questionnaire surveys. For example, it is difficult to ask about different kinds of particles and patients might also be unaware of exposure. To prove exposure to particles objectively, electron microscopy with X-ray diffraction analysis (EDXA) or X-ray diffraction spectroscopy (EDXS) have been used to detect particles in IPF lung tissue (5, 6). EDXA and EDXS are analytical methods for specific X-ray yielded by irradiation of electron beam. Investigation of 24 IPF lung tissues specimens by EDXA revealed that 18 samples contained inorganic material that was considered incidental, and two contained asbestos fibers (5). An investigation of hilar lymph nodes from IPF by EDXS showed that silicon (Si) and aluminum (Al) concentrations were high, indicating that high Si and Al concentrations may be a risk factor for the pathogenesis of IPF (6). These methods have demonstrated the existence of tissue particles objectively.

2.1. in-air micro-PIXE analysis system

In-air microparticle induced X-ray emission (in-air micro-PIXE) analysis is a method for elemental analysis of materials by irradiation with a proton microbeam. An accelerated 3.0 MeV proton beam is employed, and characteristic X-ray lines from irradiated samples are specific for various elements (7). Based on the lines obtained and their intensity, an in-air micro-PIXE system can visualize the spatial distribution of particles without microscopy and can determine the content of a very small quantity of target elements at a resolution of 1 μm with very low background noise compared to electron beam methods (8, 9). Therefore, micro-PIXE analysis has been adopted to detect the intercellular and intracellular distribution of boron and gadolinium (10) or to assess the changes of elements in the testis after cadmium exposure (11). With regard to occupational lung disease, the distribution and content of asbestos in the lungs were determined by micro-PIXE (12). One of the mechanisms of lung damage in IIP is apoptosis of cells, while the mechanism of damage in occupational lung disease also involves induction of apoptosis by inhaled agents (13, 14). Fas ligand (FasL) is a cell surface protein belonging to the tumor necrosis factor (TNF) family that binds to the Fas receptor (15). The Fas-FasL pathway is upregulated in IIP, and is essential for the occurrence of fibrosis via apoptosis (16, 17).

Currently, there is no established clinical method for assessment of the relationship between deposited particles and lung tissue damage in IIP. Such a method would be useful to assess the tissue damage caused by exposure to particles, and may help to prevent the progression of IIP. Inhalation or absorption of particles is not necessarily associated with the development of disease. To prove a relationship between exogenous agents and disease, it is

important to show that the agent induces tissue damage. Thus, a method is needed to demonstrate that particles are deposited and that tissue damage is caused by particle deposition. Although the existence of inhaled particles in IPF has been investigated by irradiation of lung tissue samples, there have been no studies about deposited particles and co-localization of protein expression in IIP lung tissues. Accordingly, the purpose of this study was to prove the relationship between deposited particles in IIP and lung tissue damage via Fas expression by employing in-air micro-PIXE analysis and immunohistochemistry.

3. METHODS

3.1. Patients and sample preparation

The diagnosis of IIP was made according to the American Thoracic Society/European Respiratory Society (ATS/ERS) International Multidisciplinary Consensus Classification of the Idiopathic Interstitial Pneumonias (18). A total twelve IIP patients (8 men and 4 women) were enrolled. Of these 12 patients, 11 patients underwent video-assisted thoracoscopic surgery (VATS), and one (patient number F12) was an autopsy case (Table 1). The diagnosis was usual interstitial pneumonia (UIP) in 9 patients (7 men and 2 women) and f-NSIP in 3 patients (2 men and 1 woman). As a control group 9 lung cancer patients (7 men and 2 women) were enrolled, and the nontumorous tissue from surgical specimens was subjected to in-air micro-PIXE analysis. For micro-PIXE analysis, paraffin-embedded lung tissue specimens were cut into sections 5 micro-m thick. Each section was dried, placed onto 10 micro-m Mylar film made from polyethylene terephthalate, and fixed in the sample holder. Then in-air micro-PIXE analysis was performed as described previously (12). This study was conducted according to the guidelines of the Declaration of Helsinki, and it was approved by the Human Research Committee of Gunma University.

3.2. In-air micro-PIXE system

A 3.0 MeV proton beam was accelerated, and then was extracted as a microbeam for micro-PIXE analysis of the characteristic X-ray lines of various elements. The X-ray lines displayed the net counts for various elements (log scale), such as Si and iron (Fe) as well as 40 other elements, and could be used to calculate the content of each element. The microbeam was focused on an area of four areas of 490 micro-m \times 490 micro-m and the 980 micro-m \times 980 micro-m image was made in each sample study. Two-dimensional analysis was used to identify the distribution and quantities of particles in that area of lung tissue, and four areas were examined in each sample. The in-air micro-PIXE system was located at the TIARA facility of the Japan Atomic Energy Agency (JAEA).

3.3. Immunohistochemistry

Lung tissue specimens were stained by anti-Fas antibody (Vision Bio, Benton Lane, UK). The specimens were incubated in 80% methanol/0.6% H₂O₂ water for 15 min, incubated in 3% H₂O₂ water for 15 min, and subsequently incubated with anti-Fas antibody (diluted \times 40) for 30 min. To develop color, ENVISION HRP⁺

Table 1. Characteristics of the study population

Patient number	Age	Sex	Smoking (pack-years)	Work	Pathological diagnosis	Distinct detected particles
F1	41	f	0	nursing	UIP	Si, Al
F2	59	m	30	service	UIP	Si
F3	63	m	43	timber	f-NSIP	Si, Fe, Mo
F4	63	f	n	clerk	UIP	Si, Fe, Mg, Al, Cu
F5	52	f	n	housewife	f-NSIP	
F6	63	m	n	service	UIP	
F7	58	m	40	painter	UIP	Si
F8	35	m	15	dealer of medicine	UIP	Si, Fe
F9	48	m	14	clerk	UIP	
F10	40	m	20	clerk	UIP	
F11	52	f	n	barber	f-NSIP	Si
F12	80	f	n	housewife	UIP	
C1	68	m	40	clerk	large cell	
C2	70	m	9	clerk	adeno	Si, Fe
C3	66	m	n	clerk	adeno	
C4	58	f	n	housewife	adeno	Si
C5	69	f	n	general store sales	adeno	
C6	70	m	20	farmer	adeno	Si
C7	56	m	7.5	service	squamous	
C8	72	m	30	farmer	adeno	
C9	60	m	5	noodle restaurant	adeno	Si

F1 to F12 the idiopathic interstitial pneumonia (IIP) patients. patients C1 to C9 are from the control group. Tissue diagnosis indicates the histological diagnosis of usual interstitial pneumonia (UIP), fibrotic-nonspecific interstitial pneumonia (f-NSIP), large cell carcinoma (large cell), adenocarcinoma (adeno), or squamous cell carcinoma (squamous).

(DAKO, Glostrup, Denmark), a horseradish peroxidase-labeled antibody, was used as the secondary antibody. Sections were examined under a BX50F4 microscope (Olympus, Tokyo, Japan), and the localization of the immunostained cells was compared with that of particles identified by in-air micro-PIXE analysis.

3.4. Calculation of the content of elements

Calculation of the content of each element was performed as described previously (12). The relation between the net counts for elements A and B was determined as follows:

$$\frac{Y_A}{Y_B} = \frac{M_B m_A \text{eff}_A \sigma_A}{M_A m_B \text{eff}_B \sigma_B}$$

where Y is the net count, M is the atomic weight of the element (amu), m is the quantity of the element in grams (g), eff is the detection efficiency for the element, and sigma is the cross-sectional area of the specific X-ray peak for the element obtained with 10 micro-m Mylar film (barns). From the above formula, the quantities of element A and element B are compared as follows:

$$\frac{m_B}{m_A} = \frac{Y_B M_B \text{eff}_A \sigma_A}{Y_A M_A \text{eff}_B \sigma_B}$$

Detection efficiency was determined when using 10 micro-m Mylar film, and the other elemental parameters (M, eff, and sigma) were as follows in this study. (a) The value of M was 32.065, 28.0855, and 55.845 for S, Si and Fe, respectively, while the value of eff was 0.181, 0.079, and 0.885, and the value of sigma was 827.927, 1012.85, and 151.7. Since the background lung tissue content was

not homogenous, sulfur (S) was used to represent the total tissue background (19). Based on the normalized X-ray data for background lung tissue, the ratio of m (the target element) to mS (m/ms) was calculated.

3.5. Statistical analysis

Data are presented as the mean \pm S.D. Differences of age and cigarette smoking between the IIP and non-IIP groups were assessed by Student's *t*-test. Differences of the mSi/mS and mFe/mS ratios between IIP and control patients were calculated by one-way ANOVA, followed by Bonferroni's comparison. Statistical analysis was performed with GraphPad Prism software and statistical significance was accepted at $*P < 0.05$.

4. RESULTS

4.1. Detection of particles

The IIP group and the control group showed no differences of age (54.5 ± 12.5 vs 62.6 ± 5.5 , mean \pm S.D.) and cigarette smoking (13.5 ± 16.5 vs 12.4 ± 14.5 pack-years, mean \pm S.D.). Lung tissue was analyzed in 12 IIP patients (patients F1 to F12) and 9 control patients (patients C1 to C9), as shown in Table 1. By two-dimensional analysis, Si was identified in 7 out of 12 patients (F1, F2, F3, F4, F7, F8, and F11) and 4 out of 9 controls (C2, C6, C7, and C9), while Fe was identified in 3 IIP patients (F3, F4, and F8) and 1 control. In patient F3, molybdenum (Mo) was detected in addition to Si, while patient F4 had magnesium (Mg), aluminum (Al), and copper (Cu) in addition to Si and Fe. In-air micro-PIXE analysis revealed Si in 7 out of 12 samples (58.3%) from IIP patients and 4 out of 9 samples (44.4%) from controls. Fe was detected in 3 out of 12 IIP samples (25%) versus only 1 out of 9

PIXE analysis of tissue particles in IIP

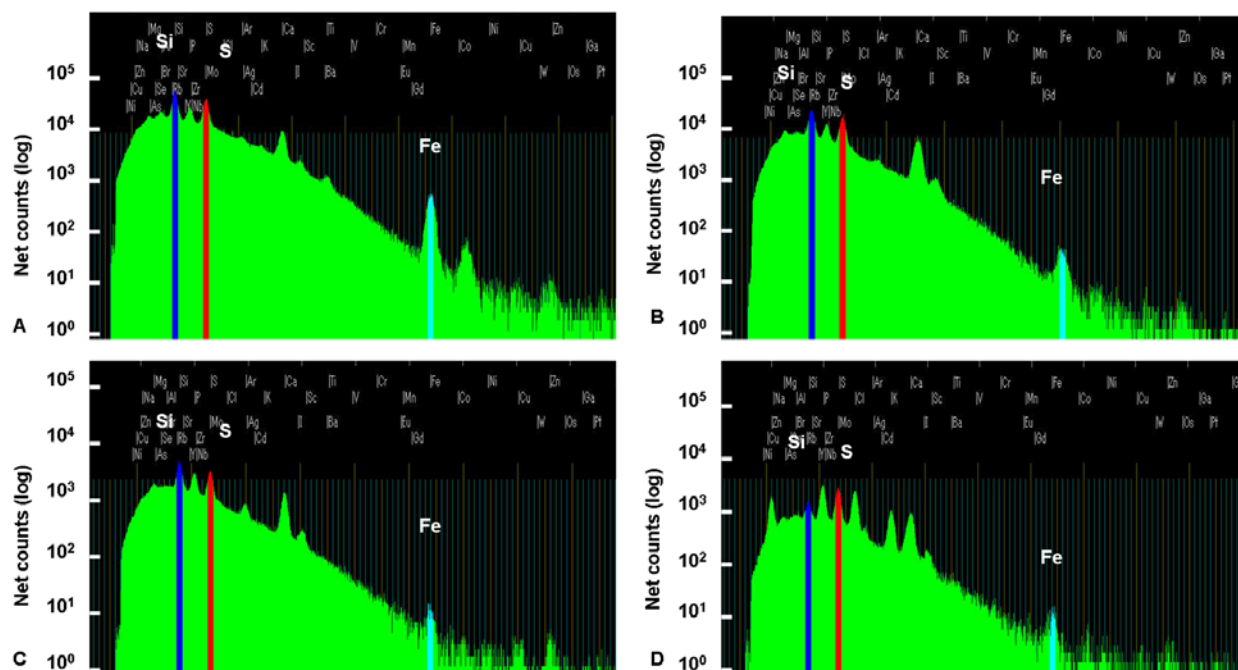


Figure 1. Representative X-ray lines obtained by microbeam analysis of lung tissue. Each spectrum line indicates the following: IIP with prominent Si and Fe deposits in patient F3 (A). IIP with little Si and Fe in patient F4 (B). IIP with little Si and Fe in patient F8 (C). A control subject (C2) with little Si and Fe (D). The peaks on the spectra display the strengths of characteristic X-ray signatures for each element, as shown by the net counts (log scale).

control samples (11.1%). In the X-ray spectrum from patient F3, the peak of Fe was higher than in other IIP patients, or controls (Figure 1). In patients F3 and F4, Fe was detected prominently. In all samples, the net counts of Si and Fe could be measured, but the particles identified from two-dimensional analysis were only observed in patients F1, F2, F3, F4, F7, F8, F11, C2, C4, C6 and C8 by in-air micro-PIXE.

4.2. Quantitative analysis of Si and Fe and the co-localization of particles with Fas expressions

Quantitative analysis of Si and Fe (relative to S) showed that the mean content of Si (1.20 ± 0.30) in IIP lungs was not significantly different from that in control lungs (1.13 ± 0.19). The content of Fe (0.027 ± 0.044) in IIP lungs was also not statistically different from that in control lungs (0.015 ± 0.0055), as shown in Figure 2. In IIP patients F3 and F4, Fe was markedly higher than the mean value for the IIP group. Immunohistochemistry revealed Fas expression by bronchial epithelial cells and interstitial lymphocytes on all IIP patients, but only two patients (F3, F4) showed co-localization of Si or Fe particles with Fas expression (Figure 3, 4). Especially in patient F3, there was co-localization of both Si and Fe with Fas expression. Some patients showed Fas expression by bronchial epithelial cells without co-localization of Si or Fe (F1, F2, F7, F8, and F11). Figure 5 displays an example of this pattern from patient F8. Other patients showed Fas expression alone (F5, F6, F9, F10, and F12) without deposition of Si or Fe. Two controls (C2 and C6) showed Fas expression by alveolar and bronchial epithelial cells,

but tiny Fe deposition was detected in a part of Fas expression area in patient C2 (Figure 6).

5. DISCUSSION

In the present study, in-air micro-PIXE analysis showed that the mean content of Si and Fe (relative to S) in lung tissue did not differ between IIP patients and non-IIP controls, with Si and Fe being detected frequently in both groups. Si was found in 7/12 IIP lungs and Fe was found in 3/12 IIP lungs by two-dimensional analysis. However only two patients showed apparently co-localization of Si and Fe deposits with Fas expression in lung tissue in IIP. In these patients, in air micro-PIXE was useful to demonstrate particle-induced tissue damage when combined with immunohistochemistry for Fas expression.

5.1. Si and Fe were detected both in IIP and non-IIP lung tissues

In a study of IIP lung tissue by X-ray diffraction analysis, Monsó reported that Si was detected 60% of IIP lungs and 68% of control lungs, while Fe was detected in 16% and 32%, respectively (5). In the present study employing in-air micro-PIXE analysis, Si was detected in 58.3% of IIP lungs and 44.4% of control lungs, while Fe was detected in 25% and 11.1%, respectively. From previous studies and our data, the detection of Si did not differ much between IIP and non-IIP patients (5). It is known that Si can be found in normal lungs, but it still needs to be determined whether these particles do not affect lung tissue or whether low-grade tissue damage occurs in

PIXE analysis of tissue particles in IIP

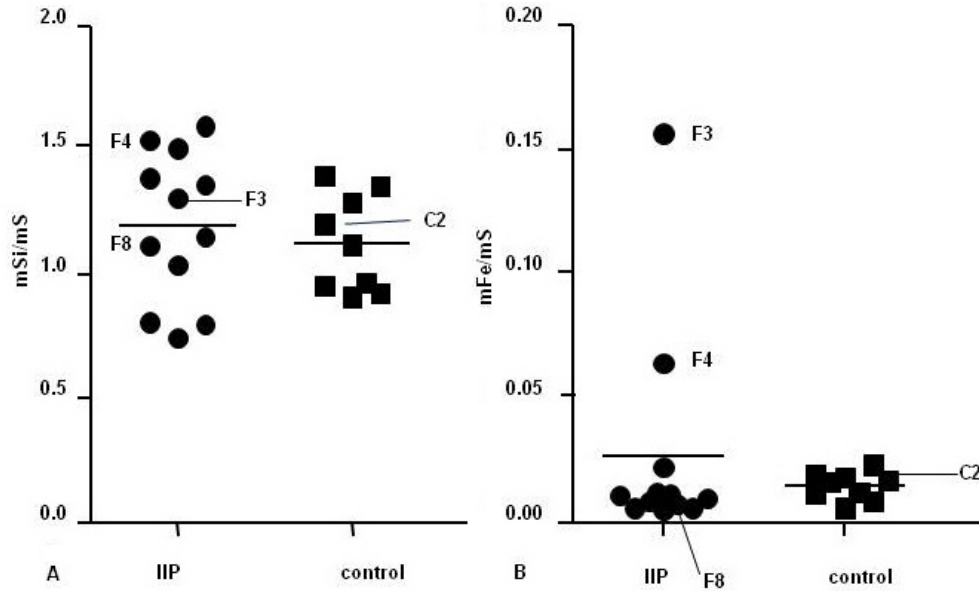


Figure 2. Quantitative elemental analysis of lung tissue by in-air micro-PIXE. The quantitative (m) ratio of Si to S (background content in lung tissue) (A) or Fe to S (B) is compared between IIP and non-IIP subjects. Each ratio was calculated as explained in the Methods section. A 980 micro-m \times 980 micro-m area of lung tissue was examined as the region of interest. Data are presented as the mean \pm S.D. for mSi/mS and mFe/mS. There were no differences between the IIP and control groups.

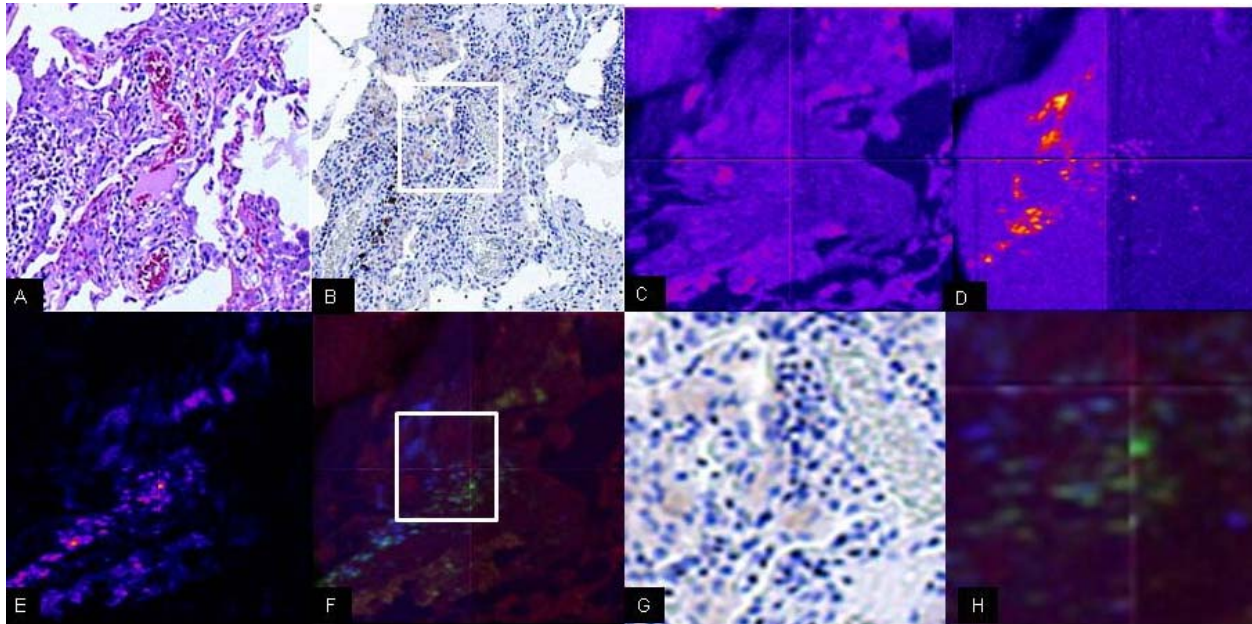


Figure 3. Immunohistochemical analysis of Fas expression and in-air micro-PIXE analysis in IIP patient F3 whose lung specimen shows high levels of Si and Fe with co-localization of Fas expression. H-E staining (A). Immunohistochemistry for Fas expression (B). In-air micro-PIXE analysis of S (C), Si (D), and Fe (E). Merged image of maps for each element (F). H-E staining shows interstitial fibrosis with infiltration of lymphocytes, indicating a diagnosis of f-NSIP (a). Immunohistochemistry shows Fas expression by brown stained interstitial lymphocytes (B). (A) and (B) \times 100. In-air micro-PIXE analysis of the same area of the lung (C, D, E, F). The content of S (C), Si (D), and Fe (E) is shown by color coding from white (high) to red (middle) and blue (low). Superimposition of S, Si, and Fe maps shows the merged pattern of each element (F): S (red), Si (blue), and Fe (green). Magnification of the areas of white square in panel (B) and (F) are shown in panel (G) and (H) \times 400. It is confirmed that particles of Si and Fe exist at the site of Fas expression.

PIXE analysis of tissue particles in IIP

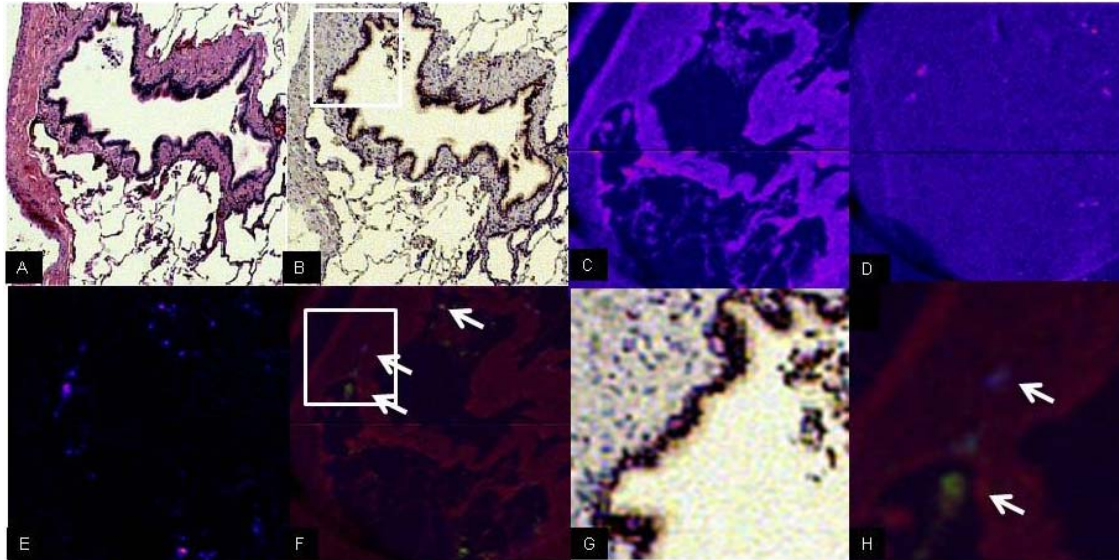


Figure 4. Immunohistochemical analysis of Fas expression and in-air micro-PIXE analysis of a lung specimen from IIP patient F4 with low levels of Si and Fe co-localized to Fas expression. H-E staining (A). Immunohistochemistry for Fas expression (B). In-air micro-PIXE analysis of S (C), Si (D), and Fe (E). Merged image of maps for each element (F). H-E staining shows interstitial fibrosis with infiltration of lymphocytes, indicating UIP (A). Immunohistochemistry shows Fas expression by brown stained interstitial lymphocytes (B). (A) and (B) $\times 100$. In-air micro-PIXE analysis of the same area of the lung (C, D, E, F). The content of S (C), Si (D), and Fe (E) is shown by color coding from white (high) to red (middle) and blue (low). Superimposition of S, Si, and Fe maps shows the merged pattern of each element (F): S (red), Si (blue), and Fe (green). Magnification of the areas of white square in panel (B) and (F) are shown in panel (G) and (H) $\times 400$. The findings confirm that few Si and Fe particles exist at the site of Fas expression.

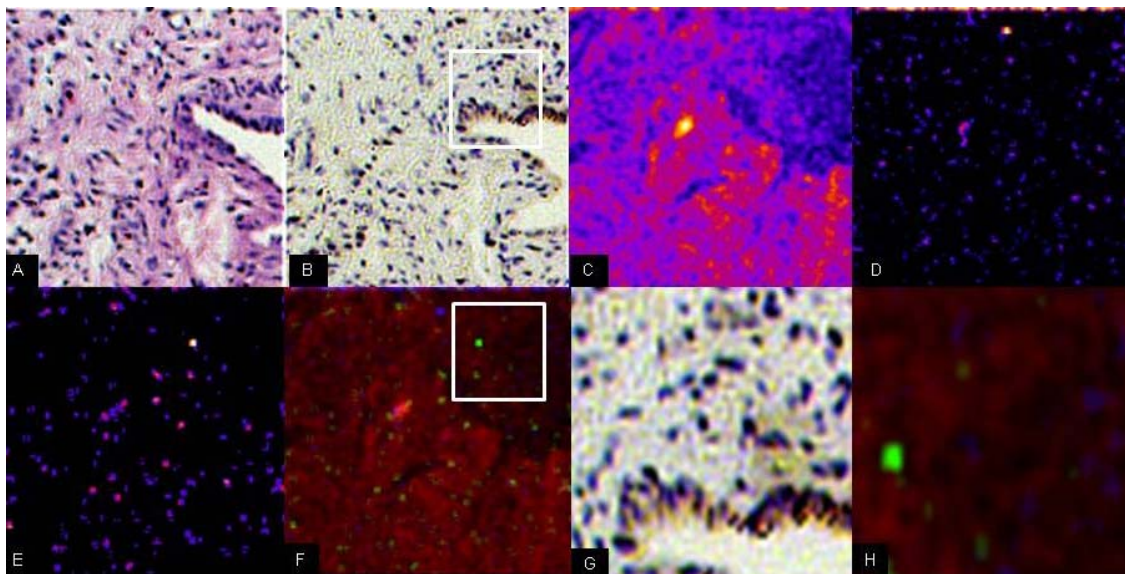


Figure 5. Immunohistochemical analysis of Fas expression and in-air micro-PIXE analysis of a lung specimen from IIP patient F8 with low levels of Si and Fe showing no co-localization to Fas expression. H-E staining (A). Immunohistochemistry for Fas expression (B). In-air micro-PIXE analysis of S (C), Si (D), Fe (E). Merged image of maps for each element (F). H-E staining shows dense interstitial fibrosis with infiltration of lymphocytes, indicating UIP (A). Immunohistochemistry shows Fas expression by brown stained epithelial cells (B). (A) and (B) $\times 100$. In-air micro-PIXE analysis of the same area of the lung (C, D, E, F). The content of S (C), Si (D), and Fe (E) is shown by color coding from white (high) to red (middle) and blue (low). Superimposition of S, Si and Fe maps shows the merged pattern of each element. Arrows indicate the sites of particles deposition (F), and each element is indicated by a different color: S (red), Si (blue), and Fe (green). Magnification of the areas of white square in panel (B) and (F) are shown in panel (G) and (H) $\times 400$. The findings confirm that Si and Fe particles were not co-localized with Fas expression.

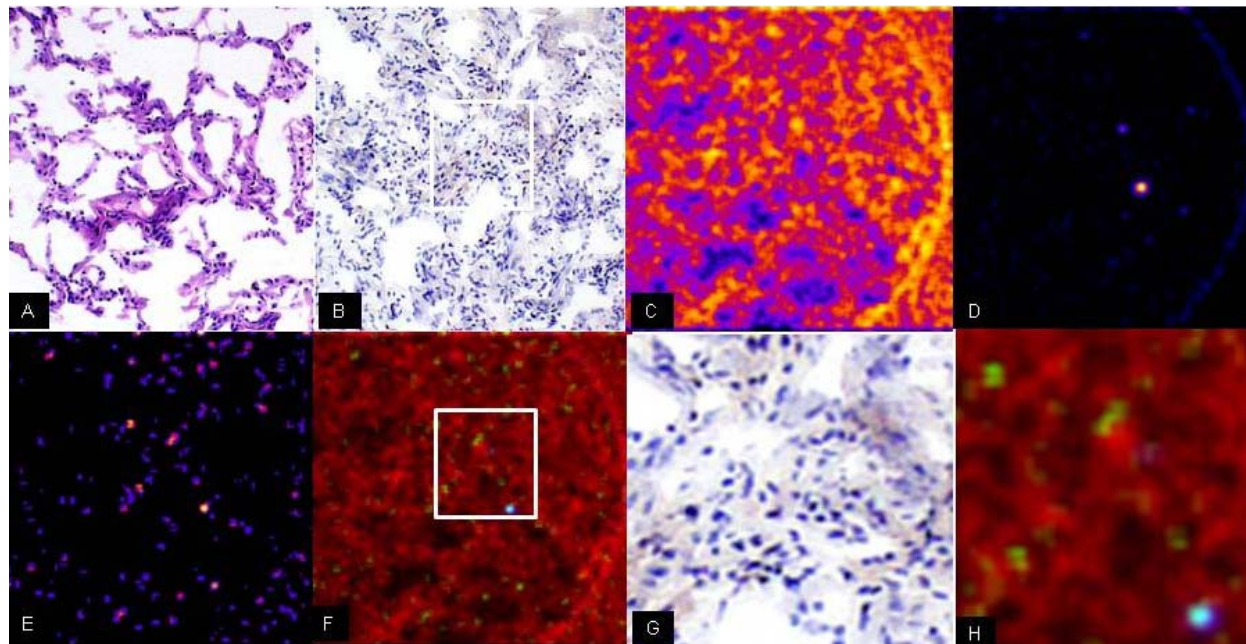


Figure 6. Immunohistochemical analysis of Fas expression and in-air micro-PIXE analysis of a lung specimen from control patient C2 with low levels of Si and Fe detected in a part of Fas expression area. H-E staining (A). Immunohistochemistry for Fas expression (B). In-air micro-PIXE analysis of S (C), Si (D), Fe (E). Merged image of maps for each element (F). H-E staining shows lymphocyte infiltration in the alveolar septae and a peripheral bronchus (A). Immunohistochemistry shows Fas expression by brown stained lymphocytes in the alveolar septa and epithelial cells (B). (A) and (B) $\times 100$. In-air micro-PIXE analysis of the same area of lung (C, D, E, F). The content of S (C), Si (D), and Fe (E) is shown by color coding from white (high) to red (middle) and blue (low). In (C), the intensity of the image has been increased so that the particles can be visualized. Note that the net count of the control lung is lower than that of other lung tissues indicated on the log scale. Superimposition of S, Si, and Fe maps shows the merged pattern of each element (F): S (red), Si (blue), and Fe (green). Magnification of the areas of white square in panel (B) and (F) are shown in panel (G) and (H) $\times 400$. The findings confirm that only a few Fe particles are detected in a part of Fas expression area.

normal lungs (20, 21). After assessment of particles in pulmonary lymph nodes from IPF patients by X-ray diffraction analysis, Kitamura reported that the content of Si and Al (relative to S) was higher in IPF patients than non-IPF subjects, but the relative Fe content to S was not different. The present study showed that the content of Si and Fe (relative to S) was not different between IIP and non-IIP lung tissues. Transportation of inhaled dust from the alveoli to regional lymph nodes by macrophages has been reported, so that the pulmonary hilar lymph nodes may better reflect the accumulation of inorganic particles compared with lung tissue (22). This might explain the different Si content of lymph node and lung tissue in the present study (6).

5.2. Co-localization of particle depositions and Fas expressions in lung of IIP patients

Only two (F3, F4) of our IIP patients showed an association of Si and Fe deposition with Fas expression. One patient was a timber worker and exposure to wood dust was reported as a strong risk factor for IPF (23, 24). Miyake found that the frequency of wood dust exposure among IPF patients was 4.9% by a questionnaire survey (3). Whether wood dust contains Si and Fe or whether there was another reason for exposure could not be

determined in this case. The risk of exposure to Si and Fe among timber workers has not been mentioned by previous reports to our knowledge. Since the present study only included 1 timber worker among 12 IIP patients (8%), we could not statistically assess the significance of being a timber worker as a risk for IPF. Smoking is also a risk factor for IPF (3). In the present study, the level of smoking and the age did not differ significantly between the IIP and non-IIP groups. Both patient F8 and patient C2 were smokers, so it is possible that smoking affects Fas expression. However, there were other smokers in the IIP and non-IIP groups whose lung tissues did not show co-localization of inhaled particles with Fas expression. It is well known that apoptosis occurs in IPF, and Fas expression may be involved in the development of IIP even if the patient has no exposure to particles (17).

5.3. Fe deposition in lung tissue

In the present study, patients F3 and F4 had higher levels of Fe compared with the other IIP patients. Iron (Fe) induces apoptosis. A questionnaire surveys have shown that metal dust (which is considered to include Fe) is an environmental risk factor for IPF (13, 23). Buerke also showed that welding fumes (containing Fe) were a risk factor of IPF by EDXA analysis (25). Asbestos bodies

PIXE analysis of tissue particles in IIP

have a high content of Fe, and we have found the colocalization of asbestos bodies and Fas expression in asbestosis patients (26). Patients F3 and F4 in the present series had no occupational exposure to asbestos based on their job history, and asbestos bodies could not be detected in bronchoalveolar lavage fluid or by tissue examination. Since iron plays a role in tissue damage via apoptosis, the high Fe content may possibly have promoted tissue damage.

5.4. Limitations of this study

Limitations of this study was a smaller patient population compared with previous studies using X-ray diffraction or questionnaire surveys, which meant that we could not statistically assess the risk of IIP in relation to Si and Fe deposition combined with Fas expression (5, 6). The Fas-FasL pathway plays an important role in the pathogenesis of IIP, but other molecules also participate in apoptosis. Furthermore, the role of genetic background in hyperreactivity to ROS was unknown (27, 28). Further analyses would be useful to determine the etiology of IIP.

Finally, we showed how in-air micro-PIXE analysis can be combined with immunohistochemical examination in IIP patients. IIP is a heterogeneous group of pulmonary diseases that feature fibrosis and the etiology has not been determined. Screening by the present method may contribute to assess the influence of particles on idiopathic interstitial pneumonia and to obtain the information for prevention of further progression of disease due to particle exposure.

6. ACKNOWLEDGEMENTS

This work was not supported by any grant. None of the authors declare competing financial interests. Y Shimizu designed this study, prepared samples, immunostained the lung tissues, irradiated, analysed the data, and wrote this manuscript. S Matsuzaki prepared the samples, analysed the data and irradiated to samples. T Satoh, T Ohkubo, A Yokoyama, Y Ishii, T Kamiya, K Arakawa prepared the sample and irradiated to sample. M Utsugi M, S Tanaka, K Shimizu prepared the samples. M Mori gave useful suggestion and discussion on this study, and K Dobashi irradiated, and gave useful suggestion on this study.

7. REFERENCES

1. MI Schwarz, TE King, G Raghu. Approach to the evaluation and diagnosis of interstitial lung disease. In: Interstitial lung disease. Eds: MI Schwarz, TE King, BC Decker Inc, London (2003)
2. K Iwai, T Mori, N Yamada, M Yamaguchi, Y Hosoda: Idiopathic pulmonary fibrosis. Epidemiologic approaches to occupational exposure. *Am J Respir Crit Care Med* 150, 670-675 (1994)
3. Y Miyake, S Sasaki, T Yokoyama, K Chida, A Azuma, T Suda, S Kudoh, N Sakamoto, K Okamoto, G Kobashi, M Washio, Y Inaba, H Tanaka: Occupational and

environmental factors and idiopathic pulmonary fibrosis in Japan. *Ann Occup Hyg* 49, 259-265 (2005)

4. VSTaskar, DB Coultas: Is idiopathic pulmonary fibrosis an environmental disease? *Proc Am Thorac Soc* 3, 293-298 (2006)

5. E Monsó, J.M. Tura, J Pujadas, F Morell, J Ruiz, J Morera: Lung dust content in idiopathic pulmonary fibrosis: a study with scanning electron microscopy and energy dispersive x-ray analysis. *Br J Ind Med* 48, 327-331(1991)

6. H Kitamura, S Ichinose, T Hosoya, T Ando, S Ikushima, M Oritsu, T Takemura: Inhalation of inorganic particles as a risk factor for idiopathic pulmonary fibrosis--elemental microanalysis of pulmonary lymph nodes obtained at autopsy cases. *Pathol Res Pract* 203, 575-585 (2007)

7. T Sakai, T Kamiya, M Oikawa, T Sato, A Tanaka, K Ishii: JAERI Takasaki in-air micro-PIXE system for various applications. *Nucl Instr And Meth In Phys Res B* 190, 271-275 (2002)

8. S Johanson. Basic principles. In: Particle-induced X-ray emission spectrometry (PIXE) chemical analysis. Eds: S Johanson, JL Campbell, KG Malmqvist, John Wiley & Sons Inc, Lund, Sweden (1995)

9. N Kozai, H Mitamura, T Ohnuki, T Sakai, T Sato, M Oikawa: Application of micro-PIXE to quantitative analysis of heavy elements sorbed on minerals. *Nucl Instr And Meth In Phys Res B* 231, 530-535 (2005)

10. K Endo, T Yamamoto, Y Shibata, K Tsuboi, A Matsumura, H Kumada, K Yamamoto, T Sakai, T Sato, M Oikawa, Y Ohara, K Ishii: Demonstration of inter- and intracellular distribution of boron and gadolinium using micro-proton-induced X-ray emission (Micro-PIXE) *Oncol. Res* 16, 57-65 (2006)

11. T Kusakabe, K Nakajima, K Nakazato, K Suzuki, H Takada, T Satoh, M Oikawa, K Arakawa, T Nagamine: Changes of heavy metal, metallothionein and heat shock proteins in Sertoli cells induced by cadmium exposure. *Toxicol In vitro* 22, 1469-1475 (2008)

12. Y Shimizu, K Dobashi, T Kusakabe, T Nagamine, M Oikawa, T Satoh, J Haga, Y Ishii, T Ohkubo, T Kamiya, K Arakawa, T Sano, S Tanaka, K Shimizu, S Matsuzaki, M Utsugi, M Mori: In-air micro-particle induced X-ray emission analysis of asbestos and metals in lung tissue. *Int J Immunopathol Pharmacol* 21, 567-576 (2008)

13. B Nemery, A Bast, J Behr, P.J. Borm, S.J.Bourke, P.H. Camus, P De Vuyst, H.M. Jansen, V.L. Kinnula, D Lison, O Pelkonen, C Saltini: Interstitial lung disease induced by exogenous agents: factors governing susceptibility. *Eur Respir J* 32, 30s-42s (2001)

14. DJ Slebos, SW Ryter, M van der Toorn, F Liu, F Guo, CJ Baty, JM Karlsson, SC Watkins, HP Kim, XWang, JS

PIXE analysis of tissue particles in IIP

Lee, DS Postma, HF Kauffman, AM Choi: Mitochondrial localization and function of heme oxygenase-1 in cigarette smoke-induced cell death. *Am J Respir Cell Mol Biol* 36, 409-417 (2007)

15. T Suda, T Takahashi, P Golstein, S Nagata. Molecular cloning and expression of the Fas ligand, a novel member of the tumor necrosis factor family. *Cell* 75, 1169-1178 (1993)

16. YP Moodley, P Caterina, AK Scaffidi, NL Misso, JM Papadimitriou, RJ McAnulty, GJ Laurent, PJ Thompson, DA Knight: Comparison of the morphological and biochemical changes in normal human lung fibroblasts and fibroblasts derived from lungs of patients with idiopathic pulmonary fibrosis during FasL-induced apoptosis. *J Pathol* 202, 486-495 (2004)

17. K Kuwano: Epithelial cell apoptosis and lung remodeling. *Cell Mol Immunol* 4, 419-429 (2007)

18. American thoracic society (ATS), and the european respiratory society (ERS) Idiopathic Pulmonary Fibrosis: Diagnosis and Treatment. International Consensus Statement. *Am J Respir Crit Care Med* 161: 646-664 (2000)

19. M Bara, P Moretto, L Razafindrabe, Y Llabador, M Simonoff, A Guet-Bara: Nuclear microanalysis of the effect of magnesium and taurine on the ionic distribution in the human amniotic membrane. *Cell Mol Biol* 42, 27-38 (1996)

20. J.P. Berry, P Henoc, P Galle, R Pariente: Pulmonary mineral dust. A study of ninety patients by electron microscopy, electron microanalysis, and electron microdiffraction. *Am J Pathol* 83, 427-456 (1976)

21. Ziskind M, Jones RN, Weill H: Silicosis. *Am Rev Respir Dis* 113, 643-665 (1976)

22. BE Lehnert, YE Valdez, CC Stewart: Translocation of particles to the tracheobronchial lymph nodes after lung deposition: kinetics and particle-cell relationships. *Exp Lung Res* 10, 245-266 (1986)

23. J Scott, I Johnston, J Britton: What causes cryptogenic fibrosing alveolitis? A case-control study of environmental exposure to dust. *BMJ* 301, 1015-1017 (1990)

24. J Mullen, MJ Hodgson, CA DeGraff, T Godar: Case-control study of idiopathic pulmonary fibrosis and environmental exposures. *J Occup Environ Med* 40, 363-367(1998)

25. U Buerke, J Schneider, J Rösler, H.J. Weitowitz: Interstitial pulmonary fibrosis after severe exposure to welding fumes. *Am J Ind Med* 41, 259-268 (2002)

26. S Matsuzaki, Y Shimizu, K Dobashi, T Nagamine, M Oikawa, T Satoh, T Ohkubo, A Yokoyama, Y Ishii, T Kamiya, K Arakawa, S Makino, M Utsugi, T Ishizuka, S

Tanaka, K Shimizu, M Mori: In-air micro-particle induced X-ray emission analysis of asbestos and metals in lung tissue. *Int J Immunopathol Pharmacol* 23, 1-11 (2010)

27. MP Steele, MC Speer, JE Loyd, KK Brown, A Herron, SH Slifer, LH Burch, MM Wahidi, JA 3rd Phillips, TA Sporn, HP McAdams, MI Schwarz, DA Schwartz: Clinical and pathologic features of familial interstitial pneumonia. *Am J Respir Crit Care Med* 172, 1146-1152 (2005)

28. TS Nawrot, E Alfaro-Moreno, B Nemery: 2008 Update in occupational and environmental respiratory disease. *Am J Respir Crit Care Med* 177, 696-700 (2007)

Key Words: Idiopathic Interstitial Pneumonia, Idiopathic Pulmonary Fibrosis, Apoptosis, Fas, Environmental Particle, Occupational Exposure, In-Air Micro-PIXE analysis

Send correspondence to: Yasuo Shimizu, Department of Medicine and Molecular Science, Gunma University Graduate School of Medicine, 3-39-15 Showa-machi, Maebashi, Gunma 371-8511, Japan, Tel: 81-27-232-5000, Fax: 81-27-232-5002; E-mail: yasuos@med.gunma-u.ac.jp

<http://www.bioscience.org/current/volE3.htm>